

LA-UR -86-980

Received by USTI

CONF-8606105--1

APR 07 1986

Los Alamos National Laboratory is operated by the University of California for the United States Department of Energy under contract W-7405-ENG-36.

LA-UR--86-980

DE36 008745

TITLE: LOW RADIOACTIVITY SPECTRAL GAMMA CALIBRATION FACILITY

AUTHOR(S): Mark A. Mathews, Geophysics Group, ESS-3
 Harry R. Bowman, Lawrence Berkeley National Laboratory
 Huang Long-ji, East China Petroleum Institute
 Morgan J. Lavelle, ECG Energy Measurements, Inc., Nevada
 Alan R. Smith, Lawrence Berkeley National Laboratory
 Joseph R. Hearst, Lawrence Livermore National Laboratory
 Harold A. Wollenberg, Jr., Lawrence Berkeley National Laboratory
 Steven Flexser, Lawrence Berkeley National Laboratory

SUBMITTED TO

Society of Professional Well Log Analysts
 Twenty-Seventh Annual Logging Symposium
 June 9-13, 1986
 Houston, Texas

MASTER

By acceptance of this article the publisher recognizes that the U.S. Government retains a nonexclusive, royalty-free license to publish or reproduce the published form of this contribution, or to allow others to do so, for U.S. Government purposes.

The Los Alamos National Laboratory requests that the publisher identify this article as work performed under the auspices of the U.S. Department of Energy.

DISTRIBUTION OF THIS DOCUMENT IS UNLIMITED

mf

Los Alamos Los Alamos National Laboratory
 Los Alamos, New Mexico 87545

LOW RADIOACTIVITY SPECTRAL GAMMA CALIBRATION FACILITY

M. A. Mathews¹, H. R. Bowman², L. Huang³, M. J. Lavelle⁴,
A. R. Smith², J. R. Hurst⁵, H. A. Wollenberg², S. Flexser²

¹Los Alamos National Laboratory, Los Alamos, NM

²Lawrence Berkeley National Laboratory, Berkeley, CA

³East China Petroleum Institute, Dongying, Shandong, People's Republic of China

⁴EG&G Energy Measurements, Inc., Las Vegas, NV

⁵Lawrence Livermore National Laboratory, Livermore, CA

ABSTRACT

A low radioactivity calibration facility has been constructed at the Nevada Test Site (NTS). This facility has four calibration models of natural stone that are 3 ft in diameter and 6 ft long, with a 12 in. cored borehole in the center of each model and a lead-shielded run pipe below each model. These models have been analyzed by laboratory natural gamma ray spectroscopy (NGRS) and neutron activation analysis (NAA) for their K, U, and Th content. Also, 42 other elements were analyzed in the NAA. The ²²²Rn emanation data were collected.

Calibrating the spectral gamma tool in this low radioactivity calibration facility allows the spectral gamma log to accurately aid in the recognition and mapping of subsurface stratigraphic units and alteration features associated with unusual concentrations of these radioactive elements, such as clay-rich zones.

INTRODUCTION

The spectral gamma logging tool measures natural gamma radiation in boreholes obtained from the elements potassium (K), uranium (U), and thorium (Th). K is determined from the 1.46 MeV gamma ray of ⁴⁰K, which constitutes 0.1% of natural K and has a 1.3 billion year half-life. Measurements are more complicated for U and Th; both elements are determined from nuclides that are members of complex decay series (Friedlander et al., 1955). U is determined from the 1.76 MeV line of ²¹⁴Bi and Th from the 2.61 MeV gamma of ²⁰⁹Tl. In addition to these gamma rays, a multitude of generally less intense gamma rays, tabulated in Erdtmann and Soyka (1979), are associated with the U and Th decay series, causing mutual interferences among the three radioelements. These interferences must be subtracted out. The spectral gamma logging tool has a NaI(Tl) detector and measures gamma rays in three energy windows as given in Table I. NaI(Tl) detectors generally have a resolution of approximately 9%, and consequently some gamma rays outside the energy window ranges are counted. These energy window ranges are listed as the fringe windows in Table I.

DISCLAIMER

This report was prepared as an account of work sponsored by an agency of the United States Government. Neither the United States Government nor any agency thereof, nor any of their employees, makes any warranty, express or implied, or assumes any legal liability or responsibility for the accuracy, completeness, or usefulness of any information, apparatus, product, or process disclosed, or represents that its use would not infringe privately owned rights. Reference herein to any specific commercial product, process, or service by trade name, trademark, manufacturer, or otherwise does not necessarily constitute or imply its endorsement, recommendation, or favoring by the United States Government or any agency thereof. The views and opinions of authors expressed herein do not necessarily state or reflect those of the United States Government or any agency thereof.

The data recorded in the energy windows (see Table II) comes from three principal sources: (1) contribution of photo peaks from the decay of nuclei for which the energy window was designed to detect, (2) contribution of photo peaks (falling at least partially in the window) from the decay of other radionuclides, and (3) contribution from Compton scattered photons (for K and U this is usually the largest). As an example of the complexity of the data recorded, the potassium energy window contains, at least partially, seven U and eight Th photo peaks along with the K photo peak. In the analysis of the spectral gamma data, it is necessary to subtract out items 2 and 3 previously listed. This subtraction can result in additional uncertainties or errors.

U has a further complication: the decay to ^{214}Bi proceeds through 75,000-year ^{230}Th and 1,600-year ^{226}Ra . The indicated half-lives for both of these intermediaries are sufficiently long to allow their separation from the ^{238}U parent by geologic processes, such as groundwater leaching, resulting in radioactive disequilibrium. If such disequilibrium has been important within the past 1 million years or less, U concentrations calculated assuming equilibrium of ^{214}Bi and ^{238}U will be in error. The Th decay nuclides have relatively short half-lives, and Th always exists in a condition of secular equilibrium within the earth.

Silicic volcanic rocks generally have the three radioelements K, U, and Th. Analyses (Quinlivan and Byers, 1977; Zielinski, 1983) for unaltered or glassy and devitrified silicic rocks of the Nevada Test Site (NTS) calc-alkaline suite generally show:

K - 20,000-50,000 ppm (2-5%),
U - 2-6 ppm, and
Th - 15-25 ppm.

Other reports (Vogel et al., 1983) show slightly higher concentrations. The Los Alamos unpublished analyses of more than 1000 samples of NTS volcanic rocks show similar ranges. The most common alteration (conversion of glass to clinopillolite) occurs in an open chemical system and generally results in the loss of K and U. This loss is generally quite small, but Th is highly immobile and not affected. There are small but significant variations of K, U, and Th within the NTS volcanic sequence due to differences among antecedent magmas and the modes of subsequent alteration. However, in alteration zones characterized by abundant kaolinite and/or smectite, large losses or depletions of K and U are found. Clays like montmorillonite are very K poor (Fertl, 1979). These known or inferred variations in K, Th, and U are evident in the spectral gamma log if the log is accurately calibrated.

DESCRIPTION OF CALIBRATION FACILITY

A facility was completed in June 1985 (Mathews et al., 1985) to accurately calibrate the spectral gamma tool for low to moderate contents of K, U, and Th in simulated borehole environments and to routinely check the calibration of this tool. Four calibration models or test pits were constructed in a building at NTS. This building has an overhead crane and a 35 ft ceiling height. Each test model, supported on a 4 ft stand, is a rock cylinder 3 ft in diameter and 6 ft in length that contains a 12 in. diameter cored borehole on axis (Figures 1, 2, and 3). The cores were drilled out at the Lawrence Berkeley Laboratory (LBL) and analyzed at the LBL low background gamma spectrometric facility and the Los Alamos National Laboratory neutron activation facility.

The four types of rock are: Sierra White (SW), Charcoal Black (CB), Lake Placid Green (LPG), and Stripa Granite (SG). The geologic descriptions and densities are given in Appendix A.

Pieces of the core for each rock type were analyzed for K, U, and Th by natural gamma ray spectroscopy (NGRS) and by neutron activation analysis (NAA). Also, 45 elements were determined from NAA (Minor et al., 1982). A listing of the 45 elements obtained from the NAA is given in Appendix B. Table III is a listing of the K, U, and Th abundances obtained from both techniques. The location of each piece of core is given in inches from the top of each rock cylinder, where 0.000 in. is the top and 72.000 in. is the bottom. The ^{222}Rn emanation data were obtained from the crushed core samples and from in situ charcoal measurements obtained in the corehole of each model. The average values for these models are also listed in Table III.

This building facility is unique because the chemical and physical characteristics of the test pits are very similar to those of the NTS drill holes logged. Grades for K, U, and Th are much lower than for any other spectral gamma calibration facility and allow greater accuracy in calibration for low count rate conditions than can be achieved elsewhere. During the calibration of a spectral gamma logging probe, lead plates are placed over the borehole after the probe has been lowered into the model leaving just enough room for the logging cable. This shielding protects the detector in the probe from cosmic ray and other background radiation.

CALIBRATION OF SPECTRAL GAMMA TOOL

Huang and Hearst (1983) have found that commercially available spectral gamma logging tools lack the required sensitivity to provide useful chemical data from NTS drill holes. Therefore, we assembled a spectral gamma tool with a large (4 x 4 x 7 in.) sodium iodide detector that overcomes the sensitivity problem. Gamma ray counts are acquired in the windows shown in Table I; these windows minimize the mutual interferences listed in Table II. The tool is calibrated by comparing count rates within the appropriate windows to the known concentrations in each test model (listed in Table III). Presently we use only three test models and do not use the counts from the LPG test model. Linear equations relate background-corrected count rates for each window to concentrations of the test models by a best-fit proportionality matrix A:

$$\text{CR}_t = A \times \text{Con}_t \quad (1)$$

where

CR_t = count rates (3 x 3 matrix) obtained from test models;
A = proportionality matrix (3 x 3 matrix); and
 Con_t = test model concentrations (3 x 3 matrix).

Once A has been determined, concentrations of K, U, and Th can be calculated from a spectral gamma log using the following matrix equation:

$$\text{Con} = \text{A}^{-1} \times \text{CR} \quad (2)$$

where

Con = concentrations calculated (3 x 1 matrix);
 A^{-1} = inverse proportionality matrix A (3 x 3 matrix) determined from calibration model data; and
 CR = field count rates from each window, raw data (3 x 1 matrix).

An example of a calibration is shown in Table IV. Removing the background from the SG, SW, and CB countrates, averaging the two ten-minute intervals, and using the NAA concentrations gives from Equation 1:

<u>Test Pits</u>	<u>Count Rates</u>					<u>Concentrations</u>			<u>Test Pits</u>
SW	K 31	U 2	Th 3	=	A	K 16050	U 0.79	Th 3.39	SW
SG	128	58.5	19			43380	32.80	33.40	SG
CB	83.5	19.5	19			39510	8.97	19.83	CB

(3)

Solving for A and its inverse, A^{-1} , allows us to use Equation 2 to convert count rates to concentrations from field data. The field data must be corrected for conditions different from those under which the calibrations were performed (Stromsewold and Wilson, 1981).

SUMMARY AND CONCLUSIONS

A low radioactivity spectral gamma calibration facility has been built from natural stone blocks at NTS. This facility consists of four calibration models of natural stone that are 3 ft in diameter and 6 ft long, with a 12 in. cored borehole in the center and a lead-shielded run pipe below each model. The radioelement concentrations determined from neutron activation analysis and natural gamma ray spectrometry are found in Table III. This facility allows the spectral gamma log to accurately aid in the recognition and mapping of subsurface stratigraphic units and alteration features such as clay-rich zones associated with unusual concentrations of these radioactive elements.

ACKNOWLEDGMENTS

This work has been supported by the United States Department of Energy and the Containment Program Office. We also wish to thank J. W. House, Containment Program Leader, for his support.

REFERENCES

- Erdtmann, G., and Soyka, W., 1979, The Gamma Rays of the Radionuclides, Verlag-Chernie, New York, Vol. 7: "Tables for Applied Gamma Ray Spectrometry," 862 p.
- Friedlander, G., Kennedy, J. W., and J. M. Miller, 1955, Nuclear and Radio-chemistry, Wiley and Sons, New York, Second Edition, 585 p.
- Fertl, W. H., 1979, "Gamma Ray Spectral Data Assists in Complex Formation Evaluation," Paper Q, Sixth European SPWLA Symposium Transactions, London, England, March, and The Log Analyst, 20, No. 5, p. 3, November/December.
- Huang, L. J. and Hearst, J. R., 1983, "Spectral Gamma Ray Logging for Clay Content," Proceedings, Second Symposium on Containment of Underground Nuclear Explosions, Kirtland AFB, Albuquerque, NM, August 2-4, and Lawrence Livermore National Laboratory Report CONF-830882, 1, p. 113-120.
- Kosanki, K. L., and Koch, C. D., 1976, "High Resolution Gamma Ray Spectroscopy Applied to Bulk Sample Analysis I," Bendix Field Engineering Report BFEC-1976-1, 68 p.
- Mathews, M. A., Warren R. G., Garcia, S. R., and Lavelle, M. J., 1985, "A Preliminary Report on NTS Spectral Gamma Logging and Calibration Models," Proceedings, Third Symposium on Containment of Underground Nuclear Explosions, Idaho Falls, ID, September 9-13, in press.
- Minor, M. M., Hensley, W. K., Denton, M. M., and Garcia, S. R., 1982, "An Automated Activation Analysis System," Journal of Radioanalytical Chemistry, 70, No. 1-2, p. 459-471.
- Quinlivan, W. D., and Byers, F. M., Jr., 1977, "Chemical Data and Variation Diagrams of Igneous Rocks from the Timber Mountain-Oasis Valley Caldera Complexes, Southern Nevada," U.S. Geological Survey Open File Report 77-724, 9 p.
- Stromswold, D. C., and Wilson, R. D., 1981, "Calibration and Data Correction Techniques for Spectral Gamma Ray Logging," in Gamma Ray Logging Workshop, February 17-19, 1981, 13 p.
- Vogel, T. A., D. C. Noble, and L. W. Younker, 1983, Chemical Evolution of a High-Level Magma System: The Black Mountain Volcanic Center, Southern Nevada, Lawrence Livermore National Laboratory Report UCRL-53444, 49 p.
- Zielinski, R. A., 1983, "Evaluation of Ash Flow Tuffs as Hosts for Radioactive Waste: Criteria Based on Selective Leaching of Manganese Oxides", U. S. Geological Survey Open File Report 83-480, 21 p.

Table I

Gamma Ray Energy Windows of Spectral Gamma Tool.

<u>Element Desired</u>	<u>Energy Window Range - MeV</u>	<u>Fringe Window Range - MeV</u>
Potassium	1.36 - 1.56	1.24 - 1.70
Uranium	1.67 - 1.87	1.52 - 2.04
Thorium	2.42 - 2.83	2.22 - 3.08

Table II

Some of the Prominent Photo Peaks Falling At Least Partially
in the Spectral Energy and Fringe Windows
(Kosanki and Koch, 1976).

Window	Energy (Kev)	Source	Decay Chain	
				Thorium
				--- Signature
				Peak
	T	2614	208 Tl	Th
	H	2448	214Bi	U
Setting	O	2204	214 Bi	U
(2420-2830)	R	Compton	Photo Peaks	U & Th
Fringe	I	Scatter	>2220	
(2220-3080)	U			
	M			
		1848	214 Bi	U
		1765	214 Bi	U
	U	1730	214 Bi	U
	R	1661	214 Bi	U
Setting	A	1631	228 Ac	Th
(1670-1870)	N	1621	212 Bi	Th
Fringe	I	1588	228 Ac	Th
(1520-2040)	U	1580	228 Ac	Th
	M	Compton	Photo Peaks	U &
		Scatter	>1520	Th
		1661	214 Bi	U
		1638	228 Ac	Th
		1631	228 Ac	Th
		1621	212 Bi	Th
		1588	228 Ac	Th
	P	1580	228 Ac	Th
	O	1509	214 Bi	U
Setting	T	1502	228 Ac	Th
(1360-1560)	A	1496	228 Ac	Th
Fringe	S	1461	40 K	K
(1240-1700)	S	1459	228 Ac	Th
	I	1408	214 Bi	U
	U	1402	214 Bi	U
	M	1378	214 Bi	U
		1281	214 Bi	U
		1238	214 Bi	U
		Compton	Photo Peaks	K, U, &
		Scatter	>1240	Th
				Potassium
				--- Signature
				Peak

Note: Contributions in windows due to pile-up are neglected.

Table III

K, U, and Th Abundances from Crushed Samples

Lake Placid Green

<u>Inches</u>	NAA			NGRS (Emanation - 5.7%)		
	<u>K (%)</u>	<u>U (ppm)</u>	<u>Th (ppm)</u>	<u>K (%)</u>	<u>U (ppm)</u>	<u>Th (ppm)</u>
9.000	0.380	0.274	0.610	0.65	0.22	0.52
22.750	0.580	0.301	0.870	--	--	-- *
27.750	0.670	0.213	0.560	0.66	0.27	0.53
32.750	0.680	0.379	0.960	0.64	0.37	0.74
38.750	0.900	0.177	0.410	0.66	0.27	0.59
45.250	0.600	0.419	1.090	0.65	0.24	0.67
64.500	0.400	0.233	0.320	0.66	0.25	0.55
-----	-----	-----	-----	-----	-----	-----
	0.601	0.285	0.689	0.65	0.27	0.60
	± 0.178	± 0.088	± 0.290	± 0.01	± 0.05	± 0.09

* -- No Sample Measured

Sierra White

<u>Inches</u>	NAA			NGRS (Emanation - 3.0%)		
	<u>K (%)</u>	<u>U (ppm)</u>	<u>Th (ppm)</u>	<u>K (%)</u>	<u>U (ppm)</u>	<u>Th (ppm)</u>
9.000	1.920	0.825	3.630	1.71	0.91	3.52
21.500	1.480	0.823	3.380	1.71	0.95	3.42
31.000	1.560	0.783	3.580	1.58	0.95	3.42
37.000	1.580	0.775	3.520	1.67	0.94	3.46
46.500	1.270	0.779	3.000	1.76	0.97	3.60
53.500	1.780	0.826	3.200	1.67	0.88	3.46
61.500	1.780	0.767	3.480	1.74	1.00	3.43
70.000	1.470	0.751	3.340	1.94	0.86	3.73
-----	-----	-----	-----	-----	-----	-----
	1.605	0.791	3.391	1.72	0.93	3.51
	± 0.210	± 0.029	± 0.210	± 0.10	± 0.05	± 0.11

Table III (continued)

Charcoal Black

<u>Inches</u>	<u>NAA</u>			<u>NGRS</u> (Emanation - 15.0%)		
	<u>K (%)</u>	<u>U (ppm)</u>	<u>Th (ppm)</u>	<u>K (%)</u>	<u>U (ppm)</u>	<u>Th (ppm)</u>
9.000	3.900	9.200	20.300	3.78	8.99	20.42
22.130	3.650	8.220	16.200	3.96	9.26	20.40
28.500	4.000	8.750	17.900	4.00	9.91	21.29
34.750	4.010	9.600	19.900	3.77	9.32	21.01
41.000	4.100	9.300	22.000	3.93	9.79	20.52
46.000	4.200	8.690	19.500	3.87	9.65	20.92
60.000	3.800	9.000	23.000	3.91	10.02	21.23
-----	-----	-----	-----	-----	-----	-----
	3.951	8.966	19.829	3.89	9.56	20.83
	± 0.185	± 0.456	± 2.309	± 0.09	± 0.38	± 0.38

Stripa Granite

<u>Inches</u>	<u>NAA</u>			<u>NGRS</u> (Emanation - 24.0%)		
	<u>K (%)</u>	<u>U (ppm)</u>	<u>Th (ppm)</u>	<u>K (%)</u>	<u>U (ppm)</u>	<u>Th (ppm)</u>
14.000	5.000	42.500	37.200	--	--	-- *
18.000	4.100	44.100	33.700	3.34	37.40	31.30
27.000	4.300	37.200	34.500	3.73	40.10	33.50
33.000	3.800	36.100	33.100	--	--	-- *
41.000	4.100	37.800	32.500	3.65	37.40	30.20
47.000	4.200	40.500	33.700	--	--	-- *
48.000	--	--	-- *	3.71	38.40	31.80
55.000	4.500	36.600	34.800	--	--	-- *
59.000	--	--	-- *	3.66	40.20	32.20
60.000	4.700	35.600	27.700	--	--	-- *
64.000	--	--	-- *	3.65	39.60	31.90
-----	-----	-----	-----	-----	-----	-----
	4.338	38.800	33.400	3.62	38.90	31.80
	± 0.381	± 3.176	± 2.704	± 0.14	± 1.40	± 1.10

0.000 in. is top of rock cylinder.
72.000 in. is bottom of rock cylinder.

* -- No Sample Measured.

Table III (continued)

The ^{222}Rn emanation data were obtained from the crushed samples from the core and from the in situ charcoal measurements obtained in the corehole of each model. The average values for these models are as follows:

Model		K (%)	U (ppm)	Th (ppm)	Emanation	Density (gm/cm ³)
SW	NAA	1.605	0.791	3.391		2.65
	NGR	1.72	0.93	3.51	3.0%	
CB	NAA	3.951	8.966	19.829		2.72
	NGR	3.89	9.56	20.83	15.0%	
LPG	NAA	0.601	0.285	0.689		2.78
	NGR	0.65	0.27	0.60	5.7%	
SG	NAA	4.338	38.800	33.400		2.63
	NGR	3.62	38.90	31.80	24.0%	

Table IV

Spectrometer Calibration Data

(Calibrations Taken on July 24, 1985)

Data in counts/second - ten minute sampling intervals in an air-filled borehole.

Mev	K 1.36-1.56	U 1.67-1.87	Th 2.42-2.83	TC1 0.2-3.012	TC2 0.4-3.012
SG	127	59	29	2859	1707
BKG	0	0	0	17	8
SG	129	58	29	2867	1703
LPG	11	0	0	121	79
BKG	0	0	0	8	6
LPG	11	0	0	121	79
SW	31	2	3	348	223
BKG	0	0	0	8	6
SW	31	2	3	348	220
CB	84	20	19	1357	841
BKG	0	0	0	14	8
CB	83	19	19	1358	841
Backgnd (Hi Air)	10	2	2	196	119
Backgnd (Lo Air)	10	2	2	194	119

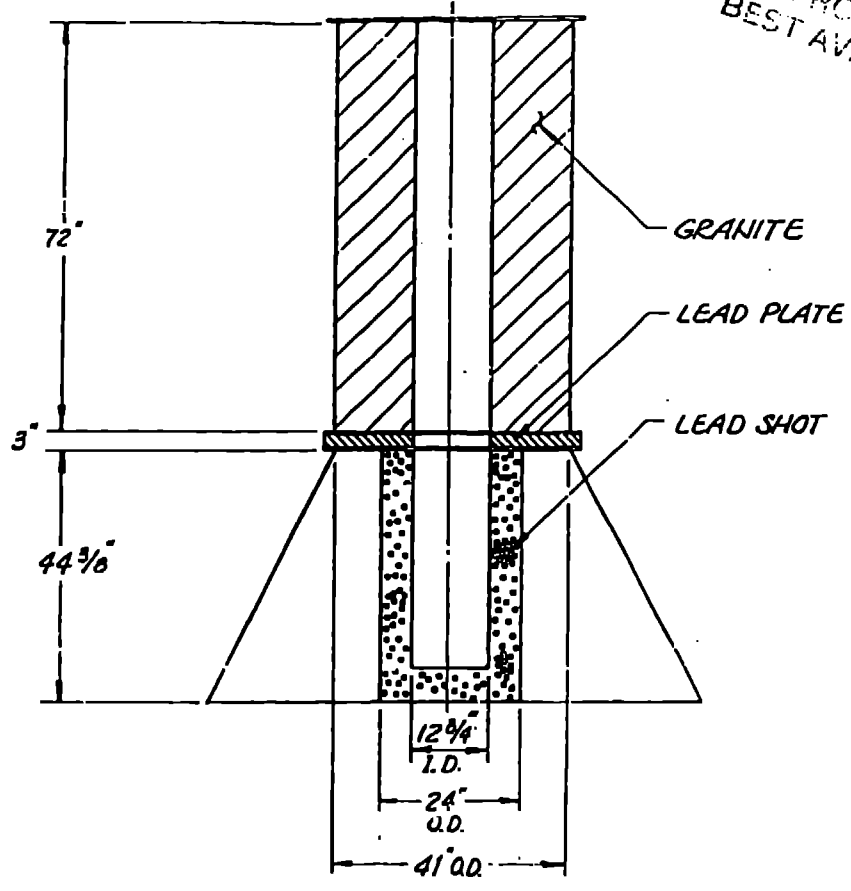
BKG - background from lead-shielded run pipe below each model.

Backgnd - tool raised to 5 ft of ceiling in Building 2201 (Hi Air), and tool lowered to 2 ft from floor in Building 2201 (Lo Air).

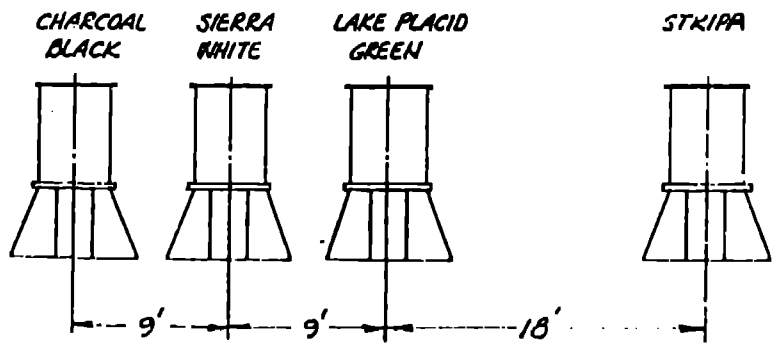
TC1 - total counts from 0.2 to 3.012 Mev

TC2 - total counts from 0.4 to 3.012 Mev

REPRODUCED FROM
BEST AVAILABLE COPY



CROSS SECTION OF A CALIBRATION CYLINDER



CYLINDER'S PLACEMENT IN BLDG.

Figure 1. Cross section of a calibration cylinder,
and placement in building at NTS.

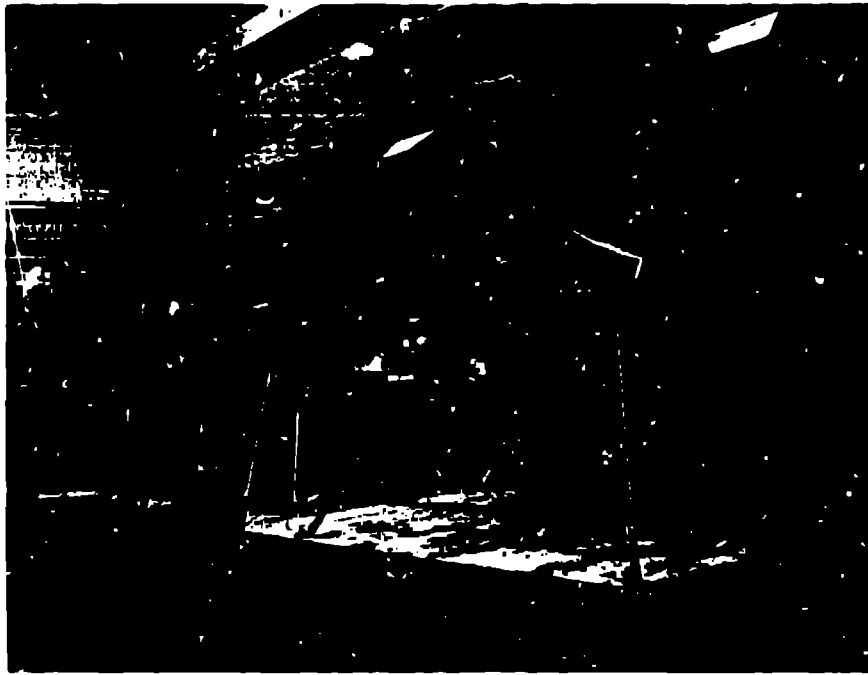


Figure 2. Photograph showing distant view of calibration models as installed.

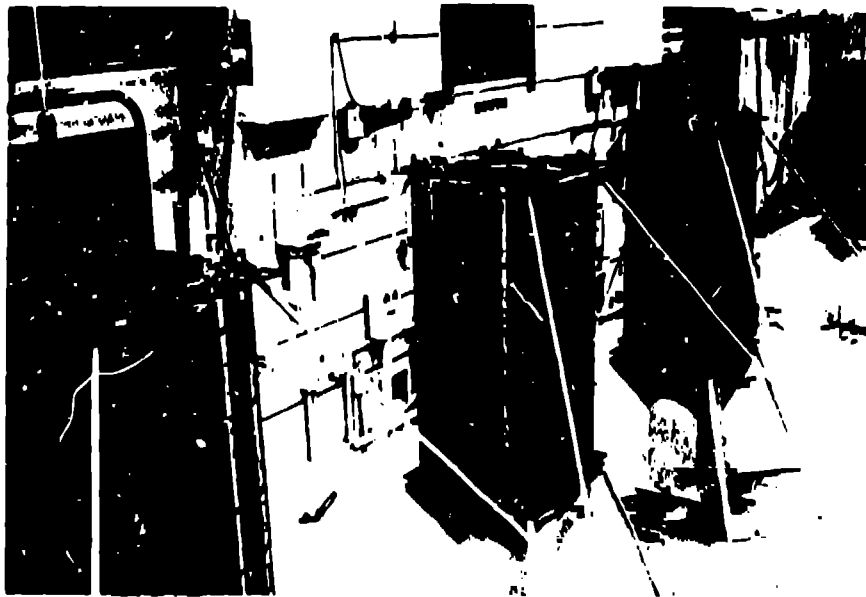


Figure 3. Photograph showing near view of calibration models as installed.

APPENDIX A

Geologic Descriptions and Densities of Lake Placid Green, Sierra White, Charcoal Black, and Stripa Granite.

Lake Placid Green

The LPG rock has an average density of 2.78 gm/cm^3 and is quarried near Au Sable Forks, New York. This rock is an anorthosite and its mineral composition is dominated by plagioclase (mainly Ca) feldspar which occurs in a fairly even-grained mosaic and constitutes approximately 90% of the rock by volume. The remainder of this rock is composed of dark, ferromagnesian minerals and their secondary alteration products. These include pyroxene, garnet, biotite, scattered grains of magnetite, and hornblende.

Sierra White

The SW rock has an average density of 2.65 gm/cm^3 and is quarried near Raymond, California. This rock is a quartz monzonite and its mineral composition is quartz, plagioclase (Na-Ca) feldspar, and alkali (K-Na) feldspar. These minerals occur in approximately equal proportions and constitute 95% of the rock by volume. The remaining portion of this rock is mainly composed of the mica minerals biotite and muscovite.

Charcoal Black

The CB rock has an average density of 2.72 gm/cm^3 and is quarried near St. Cloud, Minnesota. This rock is a quartz monzonite to granodiorite and is fairly rich in dark, ferromagnesian minerals. Feldspars and quartz comprise 80-85% of this rock by volume. Plagioclase and alkali feldspar comprise 60-65% of this rock by volume and quartz accounts for another 15-20%. The common dark minerals, in order of abundance, are hornblende, biotite, sphene, and magnetite.

Stripa Granite

The SG rock has an average density of 2.63 gm/cm^3 and is quarried near Stripa, Sweden. This rock is a quartz monzonite and is characterized by a great abundance of fractures and other deformational features. The dominant minerals, of nearly equal abundance, are quartz, plagioclase feldspar, and alkali feldspar. These minerals constitute 90-95% of the rock by volume. The remaining portion of the rock consists of the ferromagnesian minerals muscovite, chlorite, zircon and magnetite.

APPENDIX B

Listing of 45 elements obtained from the MAA of the rock blocks.

ELEMENTS	Si		LPG		SG		CB	
	Mean	Std. Dev.	Mean	Std. Dev.	Mean	Std. Dev.	Mean	Std. Dev.
Na	31050.0	772.750	29528.57	893.855	34737.0	1238.591	26885.7143	715.142
Mg	2425.0	218.763	7657.14	1089.124	3125.	575.078	9300.	1637.071
Al	75250.0	2552.310	121857.14	2544.834	84875.	3090.885	74471.4286	1549.962
Cl	106.25	7.440	144.29	7.858	148.75	30.909	284.2857	46.853
K	14050.0	2101.7	604.29	1179.914	43375.	3814.914	39500.	1848.423
Ca	16937.5	858.259	71857.14	2410.295	4550.	1063.686	21485.7143	1513.747
Ti	900.0	236.035	5000.	624.5	4250.	707.107	2552.8571	411.692
V	6.625	.518	62.	4.435	9.	1.927	54.5714	5.503
Mn	196.25	10.620	360.	52.320	225.125	38.428	404.2857	25.389
Cu	300.	0.	300.	0.	425.	88.641	300.	0.
Sr	546.25	137.002	595.71	140.577	265.	60.945	528.5714	128.248
Zn	.14	.015	.17	.012	.205	.64	.1617	.0076
As	14.25	1.488	16.57	1.678	39.625	7.347	16.7142	1.380
Se	725.	98.561	138.57	60.119	1332.5	1973.487	882.8571	40.297
Dy	.9925	.371	1.23	.257	14.325	1.281	3.1714	.198
U	.7911	.029	.2851	.088	38.8	3.174	8.9657	.456
Ga	24.38	2.825	26.71	2.289	35.	6.188	26.4285	1.718
Ag	1.58	.212	1.63	.229	3.4	.51	1.6857	.212
Ba	2.25	.668	2.26	.709	4.375	1.06	2.4285	.658
Hf	12.63	4.307	11.29	3.039	28.325	20.015	13.2	3.092
Sb	.44	.074	.43	.095	.5875	.083	.4571	.053
Te	14.5	.697	5.63	.626	31.2625	2.999	64.4571	8.312
Sm	2.24	.140	1.54	.371	9.625	1.074	8.0714	.607
Yb	.81	.181	.99	.334	8.6625	1.028	1.5142	.201
Lu	2.94	.750	3.64	.714	7.4375	3.253	3.3	1.122
Eu	.017	.003	.0169	.003	.0213	.003	.017	.003
Sc	2.40	.125	6.58	.668	5.185	.694	7.07	.768
Cr	2.11	.740	8.9286	1.775	3.2875	.724	30.	3.488
Fe	9750.	316.228	27371.4286	2632.942	14500.	1548.271	24028.5714	1306.03
Co	1.78	.601	10.9286	1.031	.5113	.409	8.3	.351
Zn	69.63	26.56	15.8285	19.767	27.875	36.487	45.5714	27.104
So	1.088	.376	1.6429	.624	4.1	1.697	2.0285	.472
Nb	64.13	6.402	12.7143	2.984	337.5	28.909	187.1428	13.704
Zr	112.	23.773	172.8571	54.989	251.25	102.730	302.8571	77.598
Ag	1.31	.351	2.2	.443	3.675	.701	1.9142	.631
Cd	1.45	.152	.4286	.091	6.4613	3.119	6.0714	.461
Ce	30.41	2.146	12.4429	3.161	79.375	4.307	133.5714	14.363
Mo	18.44	5.364	7.4	3.075	36.625	9.513	58.1428	13.68
Er	.62	.045	1.1457	.062	.4751	.069	1.44	.067
Tb	.23	.057	.3071	.184	2.465	.24	.6214	.160
La	.061	.025	.122	.033	1.7325	.074	.2508	.023
Hf	2.52	.253	.98	.198	4.6613	.249	7.0514	.473
Yb	.30	.109	.3471	.082	5.7125	1.311	1.328	.174
Hg	.81	.861	1.2571	1.1998	1.75	1.438	1.6	1.644
Tl	3.39	.710	.6886	.290	53.4	2.704	19.8285	2.309

REPRODUCED FROM
 BEST AVAILABLE COPY